Inorg. Chem. **2009**, *48*, 2760−2769

trans-Dichloro-bis-(arylazoimidazole)palladium(II): Synthesis, Structure, Photoisomerization, and DFT Calculation

P. Pratihar,[†] T. K. Mondal,[†] A. K. Patra,[‡] and C. Sinha*[,†]

Department of Chemistry, Inorganic Chemistry Section, Jadavpur University, Kolkata 700 032, India, and Inorganic and Physical Chemistry Department, Indian Institute of Science, Bangalore, India

Received July 3, 2008

Reaction between $PdCl_2$ and 1-alkyl-2-(arylazo)imidazole (RaaiR′) or 1-alkyl-2-(naphthyl-α/β-azo)imidazole (α/β-NaiR′) under reflux in ethanol has isolated complexes of compositions $Pd(RaaiR')_2Cl_2$ (**5**, **6**) and $Pd(\alpha/\beta\text{-}NaiR')_2Cl_2$ (**7**, **8**). The X-ray structure determination of one of the molecules, $Pd(\alpha\text{-}NaiBz)_2Cl_2$ (**7c**), has reported a *trans*-$PdCl_2$ configuration, and α-NaiBz acts as monodentate N(imidazole) donor ligand. The spectral (IR, UV−vis, ^{1}H NMR) data support the structure. UV light irradiation (light source: Perkin-Elmer LS 55 spectrofluorimeter, Xenon discharge lamp, $\lambda = 360-396$ nm) in a MeCN solution of the complexes shows *E*-to-*Z* isomerization of the coordinated azoimidazole unit. The reverse transformation, *Z*-to-*E*, is very slow with visible light irradiation. Quantum yields ($\phi_{E\rightarrow Z}$) of *E*-to-*Z* isomerization are calculated, and ϕ is lower than that of the free ligand but comparable with those of Cd(II) and Hg(II) complexes of the same ligand. The *Z*-to-*E* isomerization is a thermally induced process. The activation energy (E_a) of *Z*-to-*E* isomerization is calculated by controlled-temperature experimentation. *cis*-Pd(azoimidazole)Cl_2 complexes (azomidazole acts as N(imidazole) and N(azo) chelating ligand) do not respond upon light irradiation, which supports the idea that the presence of noncoordinated azo-N to make free azo (−N═N−) function is important to reveal photochromic activity. DFT calculation of $Pd(\alpha\text{-}NaiBz)_2Cl_2$ (**7c**) has suggested that the HOMO of the molecule is constituted of Pd (32%) and Cl (66%), and hence photo excitation may use the energy of Pd and Cl instead of that of the photofunctional −N═N−Ar motif; thus, the rate of photoisomerization and quantum yield decrease versus the free ligand values.

1. Introduction

Molecules that change color reversibly due to exposure to radiation of various wavelengths are defined as photochromic compounds. Recently, photochromic compounds have attracted remarkable attention due to their potential application as photonic switch devices, erasable-memory media, and optical data storage and photodrive actuators, and also in photochromic lenses, filters, smart coatings for windows and sun-blinds, specialist clothing, and jewelry.[1−5] The structural change upon light irradiation may switch on target chemical/biochemical reactions, which have immense importance in chemical research.[6] On−off switching of electron and energy transfer processes in response to external stimuli is required to communicate information at the molecular level. Photochromic compounds have been used in photoswitchable electron transfer systems and have been applied in photonic molecular devices. However, the terms photoisomerization, photochromism, and photoswitching are synonymous with a slight difference in their explicabilities: photoisomerization refers to complete structural change upon light irradiation, while photochromism is also a light-assisted

* To whom correspondence should be addressed. Fax: 91-033-2413-7121. E-mail: c_r_sinha@yahoo.com.
† Jadavpur University.
‡ Indian Institute of Science.

(1) Higashiguchi, K.; Matsuda, K.; Irie, M. *Angew. Chem., Int. Ed.* **2003**, *42*, 3537. Kume, S.; Nishihara, H. *Dalton Trans.* **2008**, 3260. Nishihara, H. *Coord. Chem. Rev.* **2005**, *249*, 1468. *Photochromism-Molecules and Systems*; Dürr, H., Bouas-Laurent, H., Eds.; Elsevier: Amsterdam, 2003.
(2) Hirschberg, J. H. K. K.; Brunsveld, L.; Ranzi, A.; Vekemans, J. A. J. M.; Sijbesma, R. P.; Meijer, E. W. *Nature* **2000**, *167*, 407.
(3) Qin, B.; Yao, R. X.; Zhao, X. L.; Tian, H. *Org. Biomol. Chem.* **2003**, *12*, 2187.
(4) Kawai, S. H.; Gilat, S. L.; Ponsinet, R.; Lehn, J.-M. *Chem.—Eur. J.* **1995**, *1*, 285.
(5) Lee, O. I. *Am. Mineral.* **1936**, *21*, 764.
(6) Tsuchiya, S. *J. Am. Chem. Soc.* **1999**, *121*, 48. Akasaka, T.; Inoue, H.; Kuwabara, M.; Mutai, T.; Otsuki, J.; Araki, K. *Dalton Trans* **2003**, 815. Otsuki, J.; Suka, A.; Yamazaki, K.; Abe, H.; Araki, Y.; Itob, O. *Chem. Commun* **2004**, 1290. Otsuki, J.; Akasaka, T.; Araki, K. *Coord. Chem. Rev.* **2008**, *252*, 32.

10.1021/ic8012365 CCC: $40.75
Published on Web 03/02/2009

Scheme 1. Isomerization of Phenylazoimidazole

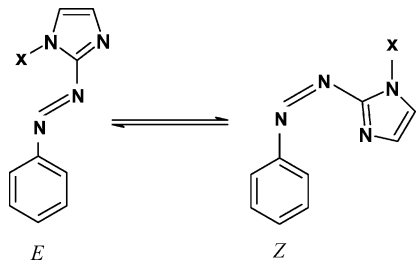

reversible structural change which returns the compound to its primary structure slowly upon switching off the source or irradiating at another wavelength zone. Photochromic materials based on extended π-electron systems such as spiropyrans, benzochromenes, spiroxazines, and azobenzenes are well-known,[7] but these molecular systems have poor long-term light and heat stability. For the development of efficient, stable photochromic performances, research on the design of organic−inorganic hybrid materials[8] is important, particularly research on materials which rise to high colorability, fast thermal or photochemical bleaching, low degradation, and so forth. The combination of a photofunctional molecule and metal ions that exhibit magnetic, optical, and electronic properties are of recent importance toward photochromic complexes.[1]

Azo-conjugated metal complexes exhibit unique properties upon light irradiation in the area of photon-mode high-density information storage photoswitching devices.[9,10] Arylazoimidazoles constitute an interesting class of heterocyclic azo compounds as a potential switching group in biological applications and in coordination chemistry, since imidazole is a ubiquitous and essential group in biology, especially as a metal coordination site. Arylazoimidazoles are known for their ability to undergo light-induced or thermal *Z*/*E* isomerization (Scheme 1). The effect of metal ions on the photochromic behavior of azoimidazoles is of current interest.[11] In this work, we study the photochromism of palladium(II)−azoimidazole complexes. So far, we have characterized Pd(azoimidazole)Cl_2 complexes with a *cis*-$PdCl_2$ configuration[12] having a chelated azoimine unit (−N═N−C═N−)Pd. Herein, we have synthesized complexes of composition *trans*-Pd(RaaiR′)$_2Cl_2$ and *trans*-Pd(α/β-NaiR′)$_2Cl_2$ (1-alkyl-2-(arylazo)imidazoles (RaaiR′) and 1-alkyl-2-(naphthyl-α/β-azo)imidazoles (α/β-NaiR′)) and have characterized them by spectroscopic techniques, and also, in one case, the structure has been confirmed by single-crystal X-ray diffraction measurement. UV light irradiation in a MeCN solution of *trans*-Pd(RaaiR′)$_2Cl_2$ and *trans*-Pd(α/β-NaiR′)$_2Cl_2$ shows *E*-to-*Z* isomerization. Quantum yields ($\phi_{E\rightarrow Z}$) of *E*-to-*Z* isomerization are calculated. The *Z*-to-*E* isomerization is a thermally induced process. The activation energy (E_a) of *Z*-to-*E* isomerization is calculated by controlled-temperature experimentation. Density functional theory (DFT) computation has been attempted to explain the photochromic efficiency of the complexes.

2. Results and Discussion

2.1. Synthesis of Complexes. 1-Alkyl-2-(arylazo)imidazoles (RaaiR′) have two potential donor centers: N(imidazole) (N) and N(azo) (N′). However, they exhibit both a bidentate chelator (N, N′)[12] and a monodentate N(imidazole) donor.[13] The ligands used in this work are 1-methyl-2-(phenylazo)imidazole (PaiMe, **1a**), 1-ethyl-2-(phenylazo)imidazole (PaiEt, **1b**), 1-benzyl-2-(phenylazo)imidazole (PaiBz, **1c**), 1-methyl-2-(*p*-tolylazo)imidazole (TaiMe, **2a**), 1-ethyl-2-(*p*-tolylazo)imidazole (TaiEt, **2b**), 1-benzyl-2-(*p*-tolylazo)imidazole (TaiBz, **2c**), 1-methyl-2-(naphthyl-α-azo)imidazole (α-NaiMe, **3a**), 1-ethyl-2-(naphthyl-α-azo)imidazole (α-NaiEt, **3b**), 1-benzyl-2-(naphthyl-α-azo)imidazole (α-NaiBz, **3c**), 1-methyl-2-(naphthyl-β-azo)imidazole (β-NaiMe, **4a**), 1-ethyl-2-(naphthyl-β-azo)imidazole (β-NaiEt, **4b**), and 1-benzyl-2-(naphthyl-β-azo)imidazole (β-NaiBz, **4c**). The reaction of Na_2PdCl_4 with RaaiR′ in an alcoholic medium or Pd(MeCN)$_2Cl_2$ and RaaiR′ in an actonitrile solution in 1:1 molar proportion has produced *cis*-Pd(RaaiR′)Cl_2.[12] Upon the addition of >2 equiv of RaaiR′ in an ethanol solution of Na_2PdCl_4 under refluxing conditions, brown-red complexes have separated that are characterized as *trans*-Pd(RaaiR′)$_2Cl_2$ (**5**, **6**) and *trans*-Pd(α/β-NaiR′)$_2Cl_2$ (**7**, **8**) (Scheme 2). The composition of the complexes has been supported by microanalytical and spectral (IR, NMR) data. The structure has been established in one case using a single-crystal X-ray diffraction study.

2.2. Molecular Structure of *trans*-Pd(α-NaiBz)$_2Cl_2$ (7c). The structure in the crystalline solid state of compound **7c** was determined by single-crystal X-ray diffraction analyses, and selected bond lengths and angles are given in Table 1. The crystal structure (Figure 1) shows that 1-benzyl-2-(naphthyl-α-azo)imidazole (α-NaiBz) behaves as a monodentate N(imidazole) donor ligand when it coordinates to Pd(II). Two α-NaiBz's coordinate in the trans configuration, and the charges are balanced by Cl in the *trans*-$PdCl_2$ orientation to form a square-planar arrangement. Arylazo-

(7) Higgins, S. *Chem. Br.* **2003**, *39*, 26. Jennifer, A.; Weller, M. T. *Chem. Commun* **2006**, 1094.
(8) Munakata, M.; Han, J.; Nabei, A.; Kuroda-Sowa, T.; Maekawa, M.; Suenaga, Y.; Gunjima, N. *Inorg. Chim. Acta* **2006**, *359*, 4281. Han, J.; Maekawa, M.; Suenaga, Y.; Ebisu, H.; Nabei, A.; Kuroda-Sowa, T.; Munakata, M. *Inorg. Chem.* **2007**, *46*, 3313.
(9) Nishihara, H. *Bull. Chem. Soc. Jpn.* **2004**, *77*, 407. Tamai, N.; Miyasaka, H. *Chem. Rev.* **2000**, *100*, 1857. Yagai, S.; Karatsu, T.; Kitamura, A. *Chem.—Eur. J.* **2005**, *11*, 4054.
(10) Irie, M. *Chem.Rev* **2000**, *100*, 1683. Ikeda, T.; Tsutsumi, O. *Science* **1995**, *268*, 1873. Kawata, S.; Kawata, Y. *Chem. Rev.* **2000**, *100*, 1777. Akitsu, T.; Einaga, Y. *Polyhedron* **2005**, *24*, 1869.
(11) Otsuki, J.; Suwa, K.; Sarker, K. K.; Sinha, C. *J. Phys. Chem. A* **2007**, *8*, 1403. Sarker, K. K.; Chand, B. G.; Suwa, K.; Cheng, J.; Lu, T.-H.; Sinha, C. *Inorg. Chem.* **2007**, *46*, 670. Sarker, K. K.; Sardar, D.; Suwa, K.; Otsuki, J.; Sinha, C. *Inorg. Chem.* **2007**, *46*, 8291.
(12) Santra, P. K.; Byabartta, P.; Chattopadhyay, S.; Falvello, L. R.; Sinha, C. *Eur. J. Inorg. Chem.* **2002**, 1124. Pal, C. K.; Chattopadhyay, S.; Sinha, C.; Bandyopadhyay, D.; Chakravorty, A. *Polyhedron* **1994**, *13*, 999. Dinda, J.; Santra, P. K.; Sinha, C.; Falvello, L. R. *J. Organomet. Chem.* **2001**, *629*, 28.
(13) Banerjee, D.; Ray, U. S.; Chantrapromma, S.; Fun, H.-K.; Lin, J.-N.; Lu, T.-H.; Sinha, C. *Polyhedron* **2005**, *24*, 1071. Ray, U. S.; Banerjee, D.; Chand, B. G.; Cheng, J.; Lu, T.-H.; Sinha, C. *J. Coord. Chem.* **2005**, *58*, 1105. Chand, B. G.; Ray, U. S.; Mostafa, G.; Lu, T.-H.; Sinha, C. *J. Coord. Chem.* **2004**, *57*, 627. Chand, B. G.; Ray, U. S.; Mostafa, G.; Lu, T.-H.; Falvello, L. R.; Sinha, C. *Polyhedron* **2003**, *22*, 3161.

Scheme 2[a]

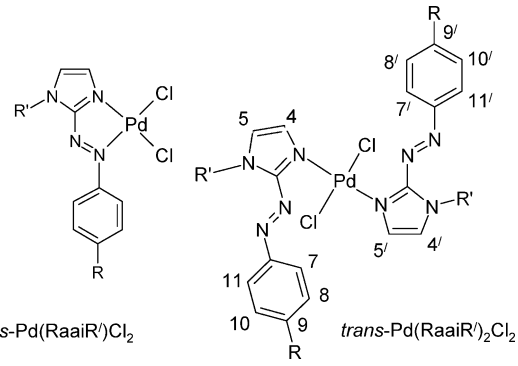

[a] *trans*-Pd(PaiMe)$_2$Cl$_2$ (**5a**), *trans*-Pd(PaiEt)$_2$Cl$_2$ (**5b**), *trans*-Pd(PaiBz)$_2$Cl$_2$ (**5c**), *trans*-Pd(TaiMe)$_2$Cl$_2$ (**6a**), *trans*-Pd(TaiEt)$_2$Cl$_2$ (**6b**), *trans*-Pd(TaiBz)$_2$Cl$_2$ (**6c**), *trans*-Pd(α-NaiMe)$_2$Cl$_2$ (**7a**), *trans*-Pd(α-NaiEt)$_2$Cl$_2$ (**7b**), *trans*-Pd(α-NaiBz)$_2$Cl$_2$ (**7c**), *trans*-Pd(*β*-NaiMe)$_2$Cl$_2$ (**8a**), *trans*-Pd(*β*-NaiEt)$_2$Cl$_2$ (**8b**), *trans*-Pd(*β*-NaiBz)$_2$Cl$_2$ (**8c**).

Table 1. Selected Bond Lengths (Å) and Angles (deg) for the Complex *trans*-Pd(α-NaiBz)$_2$Cl$_2$ (**7c**), with Estimated Standard Deviations in Parentheses

Pd(1)−N(1)	2.000(2)	C(11)−N(4)	1.413(3)
Pd(1)−Cl(1)	2.2926(16)	N(3)−N(4)	1.262(3)
C(1)−N(1)	1.368(3)	N(1)−Pd(1)−N(1[a])	180.00(15)
C(2)−N(2)	1.356(3)	N(1)−Pd(1)−Cl(1)	92.32(8)
C(3)−N(1)	1.319(3)	N(1)−Pd(1)−Cl(1[a])	87.68(8)
C(3)−N(2)	1.352(3)	Cl(1)−Pd(1)−Cl(1[a])	180.00(3)
C(3)−N(3)	1.391(3)	C(3)−N(1)−Pd(1)	126.57(16)
C(4)−N(2)	1.456(3)	C(1)−N(1)−Pd(1)	125.91(18)

[a] Symmetry transformation: $-x, -y, -z$.

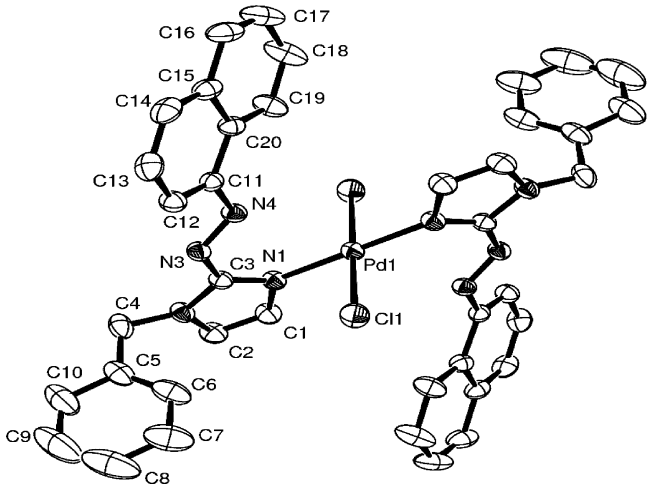

Figure 1. ORTEP view of *trans*-Pd(α-NaiBz)$_2$Cl$_2$ (**7c**), with atom labeling scheme (50% probability thermal ellipsoid).

heterocycles generally prefer N(heterocycle) and N(azo) chelation with Pd(II)[12] and Pt(II).[14] However, this is the first example in the series of azoimine functions (−N═N−C═N−) where two α-NaiBz ligands coordinate in the trans configuration, and each ligand acts as a monodentate N(imidazole) donor. The N−Pd, Cl−Pd, and N═N distances are 2.000(2), 2.2926(16), and 1.262(3) Å, respectively. The bond lengths are comparable with those of reported structures.[12,15] Pd is placed at the center of symmetry, and thus ∠N(1)−Pd−N(1*) and Cl(1)−Pd−Cl(1*) are ideal trans angles at 180.00°. The ∠Cl(1)−Pd−N(1) and ∠Cl(1*)−Pd−N(1) angles are 87.69(8) and 92.31(8)°. Thus, the square-planar structure about Pd(II) is established.

2.3. Spectral Studies. The bands in the FT-IR spectra of complexes **5**−**8** were assigned upon comparison with free ligand data and reported complexes.[12,16] Moderately intense stretchings at 1595−1600 and 1435−1445 cm^{-1} are due to ν(C═N) and ν(N═N), respectively. A moderately intense band at 335−340 cm^{-1} is assigned to ν(Pd−Cl), while *cis*-Pd(RaaiR′)Cl$_2$ gives two Pd−Cl stretches at 300−310 and 330−335 cm^{-1}.[12]

The absorption spectra were recorded in a MeCN solution in the wavelength range 250−800 nm. There are three transitions observed for **5** and **6**, while four transitions appear for **7** and **8**. The structured absorption bands around 270−290 and 360−390 nm with a molar absorption coefficient on the order of 10^4 M^{-1} cm^{-1} are assigned to $\pi\pi^*$ and $n\pi^*$ transitions (Table 2), repsectively.[11] A tail extending into 500 nm may arise from metal-orbital to ligand-orbital charge transition: dπ(Pd) → π^*(ligand). The assignment is also supported by theoretical calculations, which is described in the latter part of this paper. The photoluminescence properties of the complexes (**5**−**8**) were studied at room temperature (298 K) in a MeCN solution. The ligands (RaaiR′ and α/*β*-NaiR′) are photoinactive. The complexes Pd(RaaiR′ or α/*β*-NaiR′)$_2$Cl$_2$ exhibit emission upon excitation in the UV region (250−290 nm; Table 2). The excitation is assigned to the $\pi\pi^*$ state, which is also supported by DFT computation (vide supra). Thus, the emission observed in the complexes is the ligand-centered fluorescence (λ_{em}: 325−425 nm). Longer-wavelength ($\lambda > 500$ nm) excitation does not show emission, which indirectly supports Khasa's rule.[17]

The ^{1}H NMR spectra of *trans*-Pd(RaaiR′)$_2$Cl$_2$ are recorded in CD$_3$CN, and the signals are assigned (Table 3) unambiguously by spin−spin interaction, the effect of substitution therein, and upon comparison with previously reported data.[12,13,16] The atom numbering pattern is shown in the structure (Scheme 2). Data reveal that the signals of imidazole protons (4, 5-H) in the spectra are shifted downfield compared to the spectra of the free ligand,[12,18] while aryl protons (7-H−13-H) do not show any significant shift. This may support imidazole-N coordination to Pd(II), while azo-N may remain free. Upon light irradiation, the molecules change the structure of the coordinated azoaryl motif. The ^{1}H NMR spectra of irradiated molecules show the presence of two closely associated signals of different intensity ratios, which is distinguishable in the aliphatic region of the N-alkyl group (Figure 2), while it is difficult

(14) Pal, S.; Das, D.; Sinha, C.; Kennard, C. H. L. *Inorg. Chim. Acta* **2001**, *313*, 21.

(15) Andrade-López, N.; Alvarado-Rodríguez, J. G.; González-Montiel, S.; Rodrı´guez-Méndez, M. G.; Páez-Hernández, M. E.; Galán-Vidal, C. A. *Polyhedron* **2007**, *26*, 4825.

(16) (a) Misra, T. K. Ph. D. Thesis, Burdwan University, Burdwan, India, 1999. (b) Misra, T. K.; Das, D.; Sinha, C.; Ghosh, P. K.; Pal, C. K. *Inorg. Chem.* **1998**, *37*, 1672. (c) Dinda, J.; Pal, S.; Ghosh, B. K.; Cheng, J.; Liao, F.-L.; Lu, T.-H.; Sinha, C. *J. Coord. Chem.* **2002**, *55*, 1271.

(17) (a) Dinda, J. Ph. D. Thesis, Burdwan University, Burdwan, India, 2003. (b) Dinda, J.; Ray, U. S.; Mostafa, G.; Lu, T.-H.; Usman, A.; Razak, I. A.; Chantrapromma, S.; Fun, H.-K.; Sinha, C. *Polyhedron* **2003**, *22*, 247. (c) Dinda, J.; Bag, K.; Sinha, C.; Mostafa, G.; Lu, T.-H. *Polyhedron* **2003**, *22*, 1367.

Table 2. UV−Vis and Fluorescence Spectral Data of *trans*-Pd(RaaiR′)$_2$Cl$_2$ (**5**, **6**) and *trans*-Pd(α/β-NaiR′)$_2$Cl$_2$ (**7**, **8**)

complexes	λ_{max}/nm [10^{-3} ε (dm^3 mol^{-1} cm^{-1})]	λ_{ex}/nm	λ_{em}/nm	ϕ_f
trans-Pd(PaiMe)$_2$Cl$_2$ **5a**)	250(17.87), 360(33.44), 466(6.19)	250	327	0.021
trans-Pd(PaiEt)$_2$Cl$_2$ (**5b**)	245 (18.43), 360(30.55), 467(6.15)	245	328	0.027
trans-Pd(PaiBz)$_2$Cl$_2$ (**5c**)	252 (13.50), 374 (20.70), 481(24.95)	252	330	0.024
trans-Pd(TaiMe)$_2$Cl$_2$ **6a**)	256(14.31), 362(35.14), 472(3.93)	256	329	0.022
trans-Pd(TaiEt)$_2$Cl$_2$ (**6b**)	252(18.59), 373(74.44), 473(12.73)	252	338	0.020
trans-Pd(TaiBz)$_2$Cl$_2$ (**6c**)	255 (18.23), 370 (28.10), 478 (10.88)	255	340	0.020
trans-Pd(α-NaiMe)$_2$Cl$_2$ (**7a**)	268(14.52), 394(22.73), 411(20.95), 509(3.13)	268	375	0.048
trans-Pd(α-NaiEt)$_2$Cl$_2$ (**7b**)	270(17.21), 397(27.62), 412(25.78), 506(4.17)	270	374	0.050
trans-Pd(α-NaiBz)$_2$Cl$_2$ (**7c**)	285(19.25), 298(16.61), 378(44.39), 393(41.57), 513(6.33)	285	375	0.025
trans-Pd(β-NaiMe)$_2$Cl$_2$ (**8a**)	284(11.82), 380(32.96), 497(3.38)	284	425	0.057
trans-Pd(β-NaiEt)$_2$Cl$_2$ (**8b**)	285(11.23), 297(9.58), 381(26.02), 390(24.59), 495(6.77)	285	370	0.037
trans-Pd(β-NaiBz)$_2$Cl$_2$ (**8c**)	272(16.55), 371(37.23), 401(22.16), 501(2.03)	272	422	0.051

Table 3. ^{1}H NMR Spectral Data of UV-Light-Irradiated Solution of the Complexes (**5**−**8**) in the Aliphatic Region in Acetonitrile-d$_3$ Solution[a]

	δ, ppm (*J*, Hz)					
compd	*E*,*E*-1-CH$_3$[b]	*Z*,*Z*-1-CH$_3$[b]	*E*,*E*-1-CH$_2$	*Z*,*Z*-1-CH$_2$	*E*,*E*-(1-CH$_2$)CH$_3$[c]	*Z*,*Z*-(1-CH$_2$)CH$_3$[c]
5a	4.15	4.21				
5b			4.47[d] (10.00)	4.56[d] (10.00)	1.36(8.00)	1.41(8.00)
5c			5.55[b]	5.61[b]		
6a	4.10	4.18				
6b			4.40[d] (10.00)	4.48[d] (10.00)	1.29(8.00)	1.36(8.00)
6c			5.63[b]	5.70[b]		
7a	3.71	3.77				
7b			4.46[d] (12.00)	4.55[d] (12.00)	1.55(8.00)	1.62(8.00)
7c			5.60[b]			
8a	3.73	3.81				
8b			4.42[d] (10.00)	4.53[d] (10.00)	1.43(8.00)	1.59(8.00)
8c			5.51	5.60[b]		

[a] *E*,*E* and *Z*,*Z* refer to different isomers (Scheme 3). [b] Singlet. [c] Triplet. [d] Quartet.

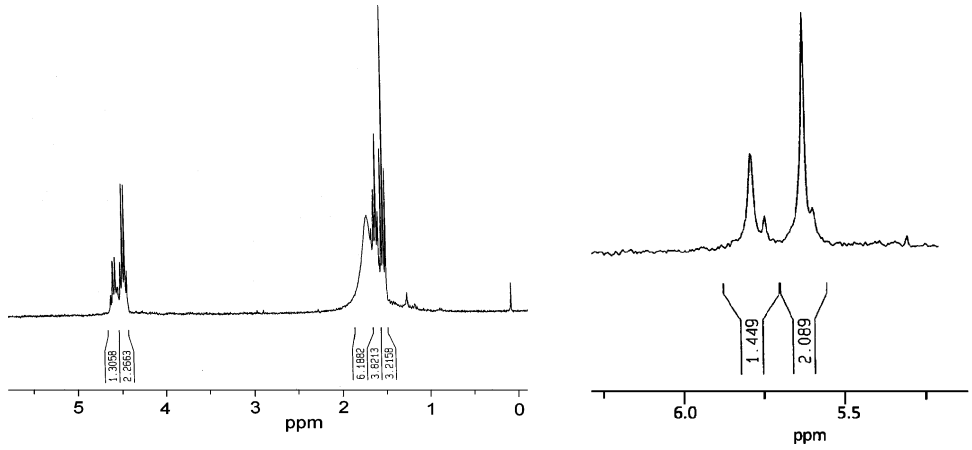

Figure 2. ^{1}H NMR (aliphatic region) of the alkyl group of *trans*-Pd(α-NaiEt)$_2$Cl$_2$ (**7b**) and *trans*-Pd(α-NaiBz)$_2$Cl$_2$ (**7c**) in acetonitrile-d$_3$ solution.

to analyze the aromatic region because of the complexity of overlapping proton signals. A lower-intensity signal appears at higher δ values (shifted by 0.05−0.15 ppm), which may be the contribution from the cis configuration of RaaiR′/NaiR′.

2.4. Photochromism of *trans*-Pd(RaaiR′)$_2$Cl$_2$ (5−8). The photoirradiation process of *trans*-Pd(RaaiR′)$_2$Cl$_2$ (**5**−**8**) complexes was followed using electronic spectroscopy. The photochromic isomerization of the free ligand was examined in a toluene solution.[11] Because of the insolubility of the complexes in toluene, the photochromic experiments were carried out in an acetonitrile solution.

Upon irradiation with UV light at λ_{max} of a MeCN solution (Table 4) of the complex, the absorption spectrum changes (Figure 3), with two and three isobestic points at ∼330 and ∼420 nm (510 nm), respectively. The intense peak at λ_{max} decreases, which is accompanied by a slight increase at the tail portion of the spectrum, 430−500 nm, until a stationary state is reached. Subsequent irradiation at the newly appearing longer-wavelength peak reverses the course of the reaction, and the original spectrum is recovered up to a point, which is another photostationary state (PSS) under irradiation at the longer-wavelength peak. The quantum yields of the *E*-to-*Z* photoisomerization were calculated, and the results are summarized in Table 4. Thermal *Z*-to-*E* isomerization rates of these complexes in MeCN at 298−313 K are collected in Table 5.

The photoisomerization of the ligand in the complexes is dependent on the nature of metal ion, its oxidation state, and its structural state.[1,19,20] The chelate complexes of these

(18) (a) Nishihara, H. *Bull. Chem. Soc. Jpn.* **2004**, *77*, 407. (b) Yutaka, T.; Mori, I.; Kurihara, M.; Mizutani, J.; Tamai, N.; Kawai, T.; Irie, M.; Nishihara, H. *Inorg. Chem.* **2002**, *41*, 7143.

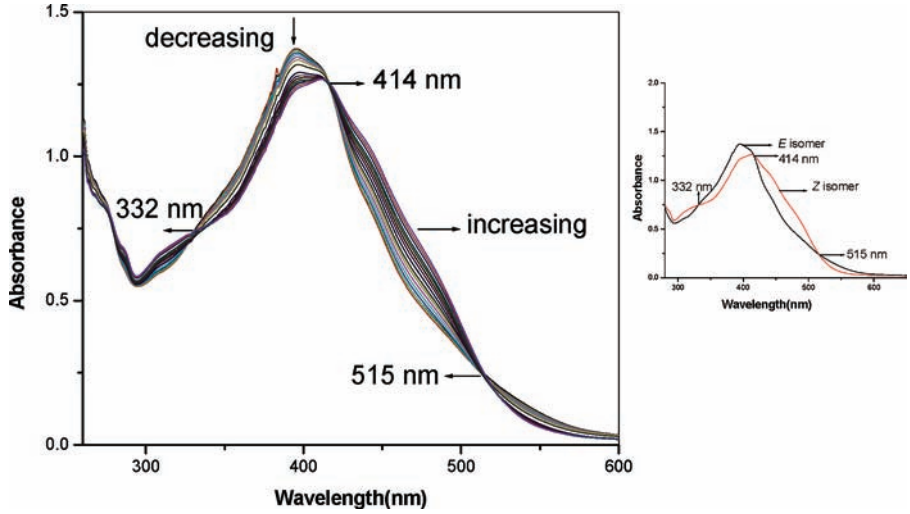

Figure 3. Spectral changes of Pd(α-NaiMe)$_2$Cl$_2$ (**7a**) in acetonitrile upon repeated irradiation at 394 nm at 3 min intervals at 25 °C. Inset figure shows spectra of *Z* and *E* isomers of the complex.

Scheme 3

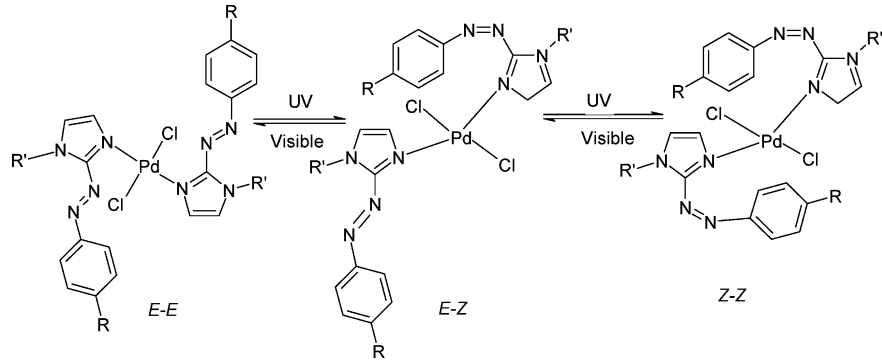

Table 4. Excitation Wavelength (λ_{π,π^*}), Rate of $E \rightarrow Z$ Conversion, and Quantum Yield ($\phi_{E\rightarrow Z}$) in MeCN

compound	λ_{π,π^*} (nm)	isobestic point (nm)	rate of $E \rightarrow Z$ conversion $\times$ 10^8 (s^{-1})	$\phi_{E\rightarrow Z}$
trans- Pd(PaiMe)$_2$Cl$_2$ (**5a**)	360	323, 432	2.354	0.123 ± 0.004
trans-Pd(PaiEt)$_2$Cl$_2$ (**5b**)	360	326, 435	2.183	0.115 ± 0.001
trans-Pd(PaiBz)$_2$Cl$_2$ (**5c**)	374	321, 433	2.001	0.110 ± 0.001
trans-Pd(TaiMe)$_2$Cl$_2$ (**6a**)	362	323, 435	2.021	0.104 ± 0.002
trans-Pd(TaiEt)$_2$Cl$_2$ (**6b**)	373	325, 435	1.983	0.095 ± 0.001
trans-Pd(TaiBz)$_2$Cl$_2$ (**6c**)	370	320, 431	1.910	0.090 ± 0.001
trans-Pd(α-NaiMe)$_2$Cl$_2$ (**7a**)	394	332, 414, 515	1.835	0.082 ± 0.002
trans-Pd(α-NaiEt)$_2$Cl$_2$ (**7b**)	396	331, 420, 525	1.051	0.046 ± 0.002
trans-Pd(α-NaiBz)$_2$Cl$_2$ (**7c**)	393	323, 424, 528	1.010	0.043 ± 0.002
trans-Pd(*β*-NaiMe)$_2$Cl$_2$ (**8a**)	380	330, 425, 530	1.770	0.058 ± 0.003
trans-Pd(*β*-NaiEt)$_2$Cl$_2$ (**8b**)	380	325, 420, 520	1.011	0.044 ± 0.002
trans-Pd(*β*-NaiBz)$_2$Cl$_2$ (**8c**)	371	325, 421, 515	1.009	0.040 ± 0.002

ligands with Pd(II) are known: *cis*-Pd(RaaiR′)Cl$_2$.[11] UV irradiation (wavelength is selected from absorption spectra) of *cis*-Pd(RaaiR′)Cl$_2$ in the solution phase (MeCN) followed by scanning of the absorption spectra does not show any observable change. This signifies a rigidity of the chelated Pd(N,N′) motif because the rotation around the N═N bond is strictly prohibited due to the coordination of the metal to the azo-N center (Scheme 2). It may be explained that the energy of the radiative wave is not sufficient to cleave the chelate ring, Pd(N,N′) at Pd−N′ (N′ refers to N(azo) center), to generate pendant N═N−Ar, which is responsible for the photoisomerization process. It, in fact, depends on the strength of the bond. It is also observed that Pt(N,N′)Cl$_2$[14] and M(N,N′)$_2$Cl$_2$ (M = Ru, Os)[16] do not show photoassisted isomerization, as is observed in Cd(RaaiR′)$_2$Cl$_2$ and Hg(RaaiR′)$_2$Cl$_2$ complexes. It is because RaaiR′ behaves as a monodentate N(imidazole) donor to Cd(II) and Hg(II) with hanging azoaryl functions.[11]

It is observed that, upon irradiation with UV light, *E*-to-*Z* photoisomerization proceeded, and the *Z* molar ratio is reached at >95% in the PSS. The absorption spectra of the *E* ligands changed with isobestic points upon excitation

(19) (a) Kepert, C. J. *Chem. Commun.* **2006**, 695. (b) Nathan, C.; Gianneschi, M.; Masar, S., III; Mirkin, C. A. *Acc. Chem. Res.* **2005**, *38*, 825.

(20) Valuer,B. *Molecular Fluorescence: Principles and Applications*; Wiley-VCH: Weinheim, Germany, 2001.

Table 5. Rate and Activation Parameters for $Z \rightarrow E$ Thermal Isomerization

compound	temp (K)	rate of thermal $Z \rightarrow E$ conversion $\times 10^4$ (s^{-1})	E_a, kJ mol^{-1}	ΔH^* kJ mol^{-1}	ΔS^* J mol^{-1} K^{-1}	ΔG^* kJ mol^{-1}
trans- $Pd(PaiMe)_2Cl_2$ (**5a**)	298	2.6329	35.55	33.01	−202.30	60.31
	303	3.6729				
	308	4.4529				
	313	5.2929				
trans-$Pd(PaiEt)_2Cl_2$ (**5b**)	298	2.4266	30.46	27.93	−220.44	65.72
	303	2.8525				
	308	3.7521				
	313	4.2619				
trans-$Pd(PaiBz)_2Cl_2$ (**5c**)	298	2.7230	34.59	32.05	−205.26	61.20
	303	3.7735				
	308	4.4929				
	313	5.3954				
trans-$Pd(TaiMe)_2Cl_2$ (**6a**)	298	2.8471	32.43	29.90	−212.31	63.30
	303	3.6429				
	308	4.4928				
	313	5.3275				
trans-$Pd(TaiEt)_2Cl_2$ (**6b**)	298	2.4125	27.39	24.85	−230.88	68.82
	303	2.7424				
	308	3.4917				
	313	4.0114				
trans-$Pd(TaiBz)_2Cl_2$ (**6c**)	298	3.0055	33.60	31.06	−208.40	62.14
	303	3.2724				
	308	4.8970				
	313	5.4118				
trans-$Pd(\alpha\text{-}NaiMe)_2Cl_2$ (**7a**)	298	2.3923	25.29	22.75	−237.77	70.88
	303	2.8398				
	308	3.3699				
	313	3.9903				
trans-$Pd(\alpha\text{-}NaiEt)_2Cl_2$ (**7b**)	298	2.3429	23.30	20.76	−244.49	72.88
	303	2.8673				
	308	3.2714				
	313	3.7823				
trans-$Pd(\alpha\text{-}NaiBz)_2Cl_2$ (**7c**)	298	2.6393	23.35	20.81	−243.57	72.60
	303	3.0398				
	308	3.6690				
	313	4.0937				
trans-$Pd(\beta\text{-}NaiMe)_2Cl_2$ (**8a**)	298	2.3643	23.64	21.10	−243.28	72.51
	303	2.9062				
	308	3.2843				
	313	3.8568				
trans-$Pd(\beta\text{-}NaiEt)_2Cl_2$ (**8b**)	298	2.4044	22.67	20.12	−246.39	73.44
	303	2.9920				
	308	3.2578				
	313	3.8801				
trans-$Pd(\beta\text{-}NaiBz)_2Cl_2$ (**8c**)	298	2.3643	24.68	22.14	−239.88	71.50
	303	2.9062				
	308	3.2843				
	313	3.8568				

(Figure 3) into the *Z* isomer and also in the case of respective complexes. The ligands and complexes show little sign of degradation upon repeated irradiation at least up to 15 cycles in each case. The quantum yields were measured for the *E*-to-*Z* ($\phi_{E\rightarrow Z}$) photoisomerization of these compounds in MeCN upon irradiation at UV wavelengths (Table 4). The $\phi_{E\rightarrow Z}$ values are significantly dependent on the nature of the substituents. The ^{1}H NMR technique has been adopted to measure the percentage composition of the irradiated solution which supports the composition obtained from absorption spectra.

Thermal *Z*-to-*E* isomerization of the complexes was followed using UV−vis spectroscopy in MeCN at different temperatures, 298−313 K. The Eyring plots in the range 298−313 K gave a linear graph, from which the activation energy was obtained (Table 5, Figure 4). The E_a values are significantly less than the free ligand values but show little difference from those of the Cd(II)− and Hg(II)−azoimidazole complexes. The rates of $E \rightarrow Z$ conversion or vise-versa also show a similar trend.[11] Additionally, *trans*-$Pd(RaaiR')_2Cl_2$ (**5**, **6**) exhibit a higher rate of transformation ($E \rightarrow Z$ or $Z \rightarrow E$) than that of *trans*-$Pd(\alpha/\beta\text{-}NaiR')_2Cl_2$ (**7**, **8**). This may be due to the larger rotor volume of **7** and **8** compared to that of **5** and **6** because of voluminous naphthyl groups in NaiR′

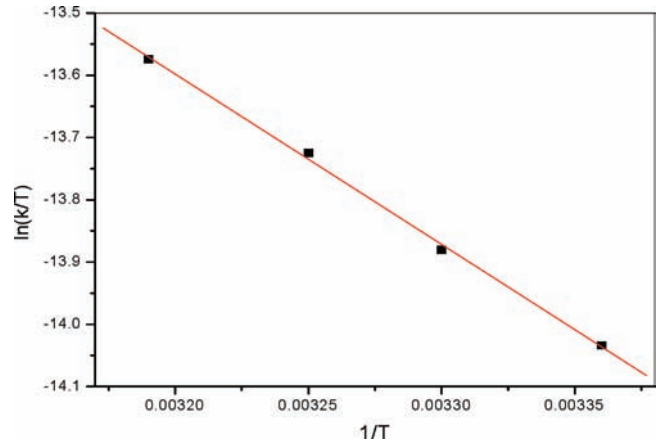

Figure 4. Eyring plot of *Z*-to-*E* thermal isomerization of $Pd(\alpha\text{-}NaiMe)_2Cl_2$.

Table 6. Cyclic Voltammogram of *trans*-Pd(RaaiR′)$_2$Cl$_2$ (**5**, **6**) and *trans*-Pd(α/*β*-NaiR′)$_2$Cl$_2$ (**7**, **8**)

compound	redox potential[a] $E_{1/2}$, V (ΔE_p, mV)		
trans-Pd(PaiMe)$_2$ Cl $_2$ (**5a**)	−0.40 (140)	−1.30[b]	−1.45[c], −1.69[b]
trans-Pd(PaiEt)$_2$Cl$_2$ (**5b**)	−0.44 (170)	−1.15[b]	−1.27[c], −1.53[b]
trans-Pd(PaiBz)$_2$ Cl$_2$ (**5c**)	−0.33 (160)	−1.08[b]	−1.25[c], −1.48[b]
trans-Pd(TaiMe)$_2$Cl$_2$ (**6a**)	−0.42 (140)	−1.24[b]	−1.32[c], −1.60[b]
trans-Pd(TaiEt)$_2$Cl$_2$ (**6b**)	−0.44 (130)	−1.25[b]	−1.32[c], −1.53[b]
trans-Pd(TaiBz)$_2$Cl$_2$ (**6c**)	−0.34 (140)	−1.23[b]	−1.30[c], −1.50[b]
trans-Pd(α-NaiMe)$_2$ Cl$_2$ (**7a**)	−0.53 (130)	−1.29[b]	−1.36[c], −1.60[b]
trans-Pd(α-NaiEt)$_2$ Cl$_2$ (**7b**)	−0.49 (160)	−1.25[b]	−1.34[c], −1.60[b]
trans-Pd(α-NaiBz)$_2$ Cl$_2$ (**7c**)	−0.46 (140)	−1.22[b]	−1.30[c], −1.63[b]
trans-Pd(*β*-NaiMe)$_2$ Cl$_2$ (**8a**)	−0.51 (130)	−1.30[b]	−1.37[c], −1.66[b]
trans-Pd(*β*-NaiEt)$_2$ Cl$_2$ (**8b**)	−0.54 (170)	−1.31[b]	−1.37[c], −1.70[b]
trans-Pd(*β*-NaiBz)$_2$ Cl$_2$ (**8c**)	−0.44 (130)	−1.25[b]	−1.37[c], −1.68[b]

[a] MeCN using Pt-disk working and Pt-wire auxiliary electrodes and reference to SCE electrode. $E_{1/2} = 0.5(E_{pa} + E_{pc})$; $\Delta E_p = ||E_{pa} - E_{pc}||$, mV. [b] E_{pc} (cathodic peak), V. [c] E_{pa} (anodic peak), V.

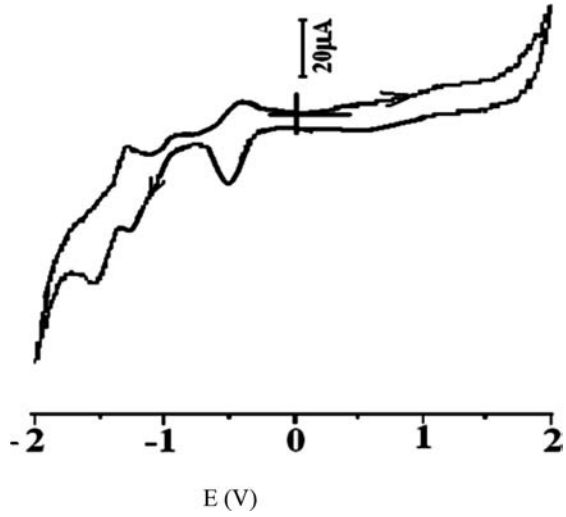

Figure 5. Cyclic voltammogram of *trans*-Pd(PaiEt)$_2$Cl$_2$. Solvent, acetonitrile; concentration of metal complex, 10^{-3} M; potential reference, saturated calomel electrode (SCE); working electrode, Pt disk; counter electrode, Pt wire; supporting electrolyte, tetrabutylammonium perchlorate (5×10^{-2} M); scan rate, 100 mV/sec; scan direction, 0 to −2V to +2V to 0; scanning of single wave required, stabilized cycle.

versus phenyl groups in RaaiR′. The entropies of activation (ΔS^*) are high and negative in Pd(II) complexes compared to that of the free ligand but lower than those of Cd(II) and Hg(II) complexes. This is also in support of an increase in rotor volume in the complexes.

2.5. Electrochemistry. The electrochemical properties of *trans*-Pd(RaaiR′)$_2$Cl$_2$ (**5**, **6**) and *trans*-Pd(α/*β*-NaiR′)$_2$Cl$_2$ (**7**, **8**) have been investigated by cyclic voltammetry. The results are given in Table 6, and a representative voltammogram is shown in Figure 5. The complexes exhibit three quasireversible ($\Delta E_p > 100$ mV) reduction couples at negative values versus a saturated calomel electrode (SCE) and are assigned to the reduction of the azo group.[11] The reduction is regarded as the electron accommodation in the LUMO characterized by azoamine functions.

2.6. Electronic Structure Calculation, Optical Spectra, and Photochromism. In this work, DFT and time-dependent DFT (TD-DFT) calculation have been performed on *trans*-Pd(α-NaiBz)$_2$Cl$_2$ (**7c**) in the gas and solution phases. The HOMO and LUMO are abbreviated as H and L, respectively, and hence so are other sets of MOs. The H (−5.44 eV) and

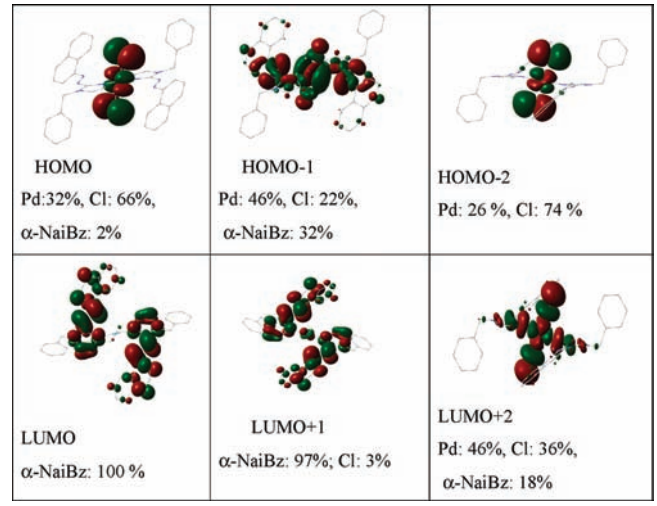

Figure 6. Some MOs of *trans*-Pd(α-NaiBz)$_2$Cl$_2$ (**7c**) along with percentage contribution of components.

H − 1 (−5.47 eV) orbitals do not differ significantly from their energies in the gas phase. These orbitals have significant Pd and Cl contributions: H, Pd(32%), Cl (66%), α-NaiBz (2%); H − 1, Pd(46%), Cl (22%), α-NaiBz (32%); H − 2, Pd(26%) and Cl(74%) (Figure 6). Other occupied MOs have a significant ligand contribution. The L (LUMO; −2.89 eV) and L + 1 (LUMO + 1; −2.82 eV) are nearly degenerate π^* orbitals of α-NaiBz. The solution-phase computation shows a similar pattern of orbital constitution and energy ordering to that in the gas phase.

To gain detailed insight into the charge transitions, the TD-DFT calculations were performed on the above complexes in the gas and acetonitrile phases (Table 7). The transitions at longer wavelengths may be considered a mixture of MLCT and XLCT [(X = Cl) → π^*(azoimine)] transitions (abbreviated in Table 7 as XLCT) along with a series of Pd-to-azoimine (MLCT) and intraligand charge-transfer (ILCT) transitions, and so forth. They are predicted to be in the range between 700 and 300 nm. High-intensity transitions ($f > 0.1$) are generally observed for XLCT and ILCT transitions. In the solution phase (MeCN), the transition energies are shifted to the higher energy side, which signifies preferential stabilization of the occupied MOs versus the unoccupied MOs, and thus energy separation increases.

In the photochromic process, UV light irradiation may be used to isomerize *E*,*E* → *E*,*Z* → *Z*,*Z* configurations (Scheme 3). Irradiation in the UV region (360−395 nm) may be responsible for the $\pi \rightarrow \pi^*$ transition. The MLCT and XLCT (X = Cl) are of a lower energetic transition which is capable of a charge transfer to azoimidazole, but the energy is insufficient to perform physical process like isomerization. Conversely, the metalated ligand may perform a charge transition (MLCT or XLCT) which is responsible for the deactivation of excited species and reduces the rate of isomerization and quantum yields (Table 4). Photoreactions tend to be deactivated in the metal-complex-attached photochromic molecules by the interaction between these two moieties. The reason for this deactivation is complicated; however, it involves both ground-state and excited-state interactions. The ground-state interaction provides low-

Table 7. Selected List of Transition Wavelength (Oscillator Strength) and Energy of Molecular Levels Calculated by the TD-DFT Method for *trans*-Pd(α-NaiBz)$_2$Cl$_2$ (**7c**)[a]

excited state	excitation energy (eV)	λ, nm ($f \times 10^3$)	major contribution
		In Gas Phase	
1	1.7592	704.7(12.2)	(75%) H − 1 → LUMO (MLCT, XLCT)
5	2.1818	568.2(8.2)	(98%) H − 2 → LUMO (MLCT, XLCT)
10	2.4547	505.0(66.1)	(20%) H − 7 → LUMO (MLCT, ILCT), (29%) H − 3 → L + 1(ILCT)
13	2.6507	467.7(54.4)	(70%) H − 4 → LUMO (ILCT)
15	2.7029	458.7(133.3)	(75%) H − 5 → L + 1 (XLCT)
17	2.7925	443.9(369.5)	(26%) H − 6 → L + 1 (XLCT), (29%) H − 3 → L + 1 (ILCT)
26	3.4526	359.1(79.7)	(51%) H − 11 → LUMO (ILCT)
27	3.4814	356.1(88.7)	(54%) H − 10 → LUMO (ILCT)
40	3.7886	327.2(256.0)	(45%) H − 13 → L + 1 (ILCT)
41	3.8145	325.0(187.1)	(35%) H − 19 → LUMO (ILCT)
		In Acetonitrile	
1	1.929	642.7(8.4)	(64%) H − 1 → LUMO (MLCT, ILCT, XLCT)
5	2.371	522.8(13.9)	(99%) H − 2 → LUMO (MLCT, XLCT)
8	2.728	454.4(75.4)	(27%) H − 3 → L + 1 (ILCT), (21%) H − 7 → LUMO (MLCT, ILCT)
11	2.974	416.9(173.4)	(84%) H − 4 → LUMO (ILCT)
13	3.026	409.6(259.4)	(54%) H − 3 → L + 1 (ILCT)
17	3.138	395.0(29.9)	(45%) H − 5 → L + 1, (33%) H − 6 → L + 1 (XLCT)
25	3.682	336.6(45.0)	(42%) H − 10 → LUMO, (32%) H − 11 → L + 1 (ILCT)
26	3.792	326.9(66.8)	(28%) H − 12 → LUMO, (21%) H − 8 → L + 1 (ILCT)
29	3.851	321.9(58.1)	(40%) H − 12 → LUMO (ILCT)

[a] XLCT: π(Cl) → π^*(azoimine). MLCT: dπ(Pd) → π^*(azoimine). ILCT: π(azoimine) → π^*(azoimine).

energy routes in the thermal isomerization and involves distortion of the π conjugation. Metal complexes often have a low-energy excited state and promote intersystem crossing to decrease the quantum efficiency of the photoreaction.[1] DFT calculation of one of the complexes, *trans*-Pd(α-NaiBz)$_2$Cl$_2$ (**7c**), shows a high population of Pd (32%) and Cl (66%) in the HOMO. The photoexcitation may use the energy of Pd and Cl instead of that of the photofunctional arylazo unit; thus, the rate of photoisomerization decreases versus the free ligand values. Additionally, the rotor volume has a significant effect leading to regulation of the rate and quantum efficiency of the process.

3. Experimental Section

3.1. Materials. $PdCl_2$ was obtained from Arrora Matthey, Kolkata, India. 1-Alkyl-2-(arylazo)imidazoles were synthesized according to a reported procedure.[11] All other chemicals and solvents were reagent-grade as received.

3.2. Physical Measurements. Microanalytical data (C, H, N) were collected on a Perkin-Elmer 2400 CHNS/O elemental analyzer. Spectroscopic data were obtained using the following instruments: UV−vis spectra from a Perkin-Elmer Lambda 25 spectrophotometer and IR spectra (KBr disk, 4000−200 cm^{-1}) from Perkin-Elmer RX-1 and JASCO model 420 FTIR spectrophotometers. Photoexcitation has been carried out using a Perkin-Elmer LS-55 spectrofluorimeter and ^{1}H NMR spectra from a Bruker (AC) 300 MHz FTNMR spectrometer.

Emission was examined using an LS 55 Perkin-Elmer spectrofluorimeter at room temperature (298 K) in MeCN under degassed conditions. Electrochemical measurements were performed using computer-controlled PAR model 270 VERSASTAT electrochemical instruments with Pt-disk electrodes. All measurements were carried out under a nitrogen environment at 298 K with reference to a SCE in acetonitrile using [nBu$_4$N][ClO$_4$] as a supporting electrolyte. The reported potentials are uncorrected for junction potential.

The luminescence property was measured using an LS-55 Perkin-Elmer fluorescence spectrophotometer at room temperature (298 K) in CH_3CN solution with a 1-cm-path-length quartz cell. The fluorescence quantum yield of the complexes was determined using naphthalene as a reference. The fluorescence quantum yield of the reference is 0.21 in MeCN. The complex and the reference dye were excited at 230−290 nm.[20] The complex and the reference dye were excited, maintaining nearly equal absorbance (∼0.1), and the emission spectra were recorded. The area of the emission spectrum was integrated using the software available in the instrument, and the quantum yields were calculated according to the following equation:

$$\phi_S/\phi_R = [A_S/A_R] \times [(Abs)_R/(Abs)_S] \times [\eta_S^2/\eta_R^2]$$

Here, ϕ_S and ϕ_R are the fluorescence quantum yields of the sample and the reference, respectively, A_S and A_R are the area under the fluorescence spectra of the sample and the reference, respectively, $(Abs)_S$ and $(Abs)_R$ are the respective optical densities of the sample and the reference solution at the wavelength of excitation, and η_S and η_R are the values of the refractive index for the solvent used for the sample and the reference, respectively.

3.3. Synthesis of *trans*-Pd(α-NaiEt)$_2$Cl$_2$. To an 80 mg (0.27 mmol) ethanolic solution of Na_2PdCl_4 was added 170 mg (0.68 mmol) of α-NaiEt, which was then stirred for 0.5 h and refluxed for 3−4 h. The brown-red solution was kept in a beaker. After solvent evaporation, the solid mass was crystalized by the diffusion of the CH_2Cl_2 solution in the hexane layer.

Microanalytical data. Calcd for $C_{20}H_{20}N_8Cl_2Pd$ (**5a**): C, 43.71; H, 3.64; N, 20.40. Found: C, 43.81; H, 3.60; N, 20.50%. Calcd for $C_{22}H_{24}N_8Cl_2Pd$ (**5b**): C, 45.75; H, 4.16; N, 19.41. Found: C, 45.84; H, 4.20; N, 19.35%. Calcd for $C_{32}H_{28}N_8Cl_2Pd$ (**5c**): C, 54.75; H, 3.99; N, 15.96. Found: C, 54.81; H, 4.05; N, 16.03%. Calcd for $C_{22}H_{24}N_8Cl_2Pd$ (**6a**): C, 45.75; H, 4.16; N, 19.41. Found: C, 45.70; H, 4.22; N, 19.59%. Calcd for $C_{24}H_{28}N_8Cl_2Pd$ (**6b**): C, 47.60; H, 4.63; N, 18.51. Found: C, 47.70; H, 4.68; N, 18.40%. Calcd for $C_{34}H_{32}N_8Cl_2Pd$ (**6c**): C, 55.93; H, 4.38; N, 15.35. Found: C, 54.00; H, 4.45; N, 15.27%. Calcd for $C_{28}H_{24}N_8Cl_2Pd$ (**7a**): C, 51.77; H, 3.69; N, 17.26. Found: C, 51.70; H, 3.65; N, 17.32%. Calcd for $C_{30}H_{28}N_8Cl_2Pd$ (**7b**): C, 53.17; H, 4.13; N, 16.54. Found: C, 53.24; H, 4.10; N, 16.50%. Calcd for $C_{40}H_{32}N_8Cl_2Pd$ (**7c**): C, 59.92; H,

Table 8. Selected Crystallographic Data for [*trans*-Pd(α-NaiBz)$_2$Cl$_2$] (**7c**)

	trans-Pd(α-NaiBz)$_2$Cl$_2$ (**7c**)
formula	$C_{40}H_{32}Cl_2N_8Pd$
fw, g M^{-1}	802.04
cryst syst	monoclinic
space group	$P2_1/c$ (No. 14)
T, K	293
a, Å	10.854(11)
b, Å	14.099(14)
c, Å	12.228(12)
β, deg	93.729(18)
V, Å^3	1867(3)
Z	2
density (calculated) (Mg/m^3)	1.426
λ, Å (Mo Kα)	0.71073
abs coeff (mm^{-1})	0.680
data/restraints/params	4420/0/288
goodness-of-fit on F^2	1.024
R (F_o)^a [$I > 2\sigma(I)$]	0.0351
wR (F_o)^b [$I > 2\sigma(I)$]	0.0752
R [all data] (wR [all data])	0.0574 (0.0831)
largest difference in peak and hole (e Å^{-3})	0.330, −0.257
weight factor: $w = 1/[\sigma^2(F_o^2) + (AP)^2 + (BP)]$	$A = 0.0381$; $B = 0.2712$

^{a} $R = \sum||F_o| - ||F_c||/\sum|F_o|$. ^{b} $wR = \{\sum[w(F_o^2 - F_c^2)^2]/\sum[w(F^2_o)^2]\}^{1/2}$; $w = [\sigma^2(F_o)^2 + (AP)^2 + BP]^{-1}$, where $P = (F_o^2 + 2F_c^2)/3$.

3.99; N, 13.98. Found: C, 59.96; H, 3.90; N, 13.88%. Calcd for $C_{28}H_{24}N_8Cl_2Pd$ (**8a**): C, 51.77; H, 3.69; N, 17.26. Found: C, 51.72; H, 3.63; N, 17.20%. Calcd for $C_{30}H_{28}N_8$ Cl_2Pd (**8b**): C, 53.17; H, 4.13; N, 16.54. Found: C, 53.10; H, 4.10; N, 16.50%. Calcd for $C_{40}H_{32}N_8Cl_2Pd$ (**8c**): C, 59.92; H, 3.99; N, 13.98. Found: C, 59.98; H, 3.95; N, 14.04%.

3.4. X-Ray Diffraction Study of *trans*-Pd(α-NaiBz)$_2$Cl$_2$ (7c). The crystallographic data are shown in Table 8. A suitable single crystal of *trans*-Pd(α-NaiBz)$_2$Cl$_2$ (**7c**) (0.60 × 0.30 × 0.15 mm) was mounted on a CCD diffractometer equipped with fine-focus sealed-tube graphite monochromated Mo Kα ($\lambda = 0.71073$ Å) radiation. The unit cell parameters and crystal-orientation matrices were determined by least-squares refinements of all reflections. The intensity data were corrected for Lorentz and polarization effects, and an empirical absorption correction was also employed using the Bruker SAINT program.[21] Data were collected applying the condition $I > 2\sigma(I)$. Out of a total of 16 034 data points, 4420 were used within hkl parameters $-14 \le h \le 14$, $-18 \le k \le 18$, and $-16 \le l \le 16$ for structure solution. All of these structures were solved by direct methods and followed by successive Fourier and difference Fourier syntheses. Full-matrix least-squares refinements on F^2 were carried out using SHELXL-97 with anisotropic displacement parameters for all non-hydrogen atoms. Hydrogen atoms were constrained to ride on the respective carbon or nitrogen atoms with isotropic displacement parameters equal to 1.2 times the equivalent isotropic displacement of their parent atom in all cases of aromatic units. All calculations were carried out using the SHELXS 97,[22] SHELXL 97,[23] PLATON 99,[24] and ORTEP-3[25] programs.

3.5. Photometric Measurements. Absorption spectra were taken with a PerkinElmer Lambda 25 UV/vis spectrophotometer in a 1 × 1 cm quartz optical cell maintained at 25 °C with a Peltier thermostat. The light source of a PerkinElmer LS 55 spectrofluorimeter was used as an excitation light, with a slit width of 10 nm. An optical filter was used to cut off overtones when necessary. The absorption spectra of the Z isomers were obtained by extrapolation of the absorption spectra of a Z-rich mixture for which the composition was known from ^{1}H NMR integration. Quantum yields (ϕ) were obtained by measuring initial E-to-Z isomerization rates (ν) in a well-stirred solution within the above instrument using the equation

$$\nu = (\phi I_0/V)(1 - 10^{-\mathrm{Abs}})$$

where I_0 is the photon flux at the front of the cell, V is the volume of the solution, and Abs is the initial absorbance at the irradiation wavelength. The value of I_0 was obtained by using azobenzene ($\phi = 0.11$ for $\pi-\pi^*$ excitation[26]) under the same irradiation conditions.

The thermal Z-to-E isomerization rates were obtained by monitoring absorption changes intermittently for a Z-rich solution kept in the dark at constant temperatures (T) in the range from 298 to 313 K. The activation energy (E_a) and the frequency factor (A) were obtained from the Arrhenius plot

$$\ln k = \ln A - E_a/RT$$

where k is the measured rate constant, R is the gas constant, and T is the temperature. The values of activation free energy (ΔG^*) and activation entropy (ΔS^*) were obtained through the relationships

$$\Delta G^* = E_a - RT - T\Delta S^* \text{ and}$$

$$\Delta S^* = [\ln A - 1 - \ln(k_B T/h)/R]$$

where k_B and h are Boltzmann's and Plank's constants, respectively.

3.6. DFT Calculations. DFT calculations were carried out using X-ray crystallographic parameters of complex **7c**. A Gaussian 03w package[27] was run on a personal computer. The functional B3LYP[28] and basis set LanL2DZ[29] were chosen for the calculations. The electronic spectrum was calculated using TD-DFT methods. For nonmetallic atoms, diffuse and polarization functions were used. Natural bond order (NBO) calculations were performed with the NBO code included in Gaussian 03.

4. Conclusion

trans-Dichloro-bis-(azoimidazole)palladium(II) complexes of 1-alkyl-2-(arylazo)imidazoles are described. One of the complexes has been characterized by single-crystal X-ray structure study. Photochromisms of the complexes are examined using UV light irradiation in a MeCN solution. Quantum yields of E-to-Z isomerization are determined in

(21) *SMART*; *SAINT*; Bruker AXS Inc: Madison, WI, 1998.
(22) Sheldrick, G. M. *SHELXS 97*; University of Gottingen: Gottingen, Germany, 1997.
(23) Sheldrick, G. M. *SHELXL 97*; University of Gottingen, Gottingen, Germany, 1997.
(24) Spek, A. L. *PLATON*; University of Utrecht: Utrecht, The Netherlands, 1999.
(25) Farrugia, L. J. *J. Appl. Crystallogr.* **1997**, *30*, 565.
(26) Zimmerman, G.; Chow, L.; Paik, U. *J. Am. Chem. Soc.* **1958**, *80*, 3528.
(27) Frisch, M. J.; Trucks, G. W.; Schlegel, H. B.; Scuseria, G. E.; Robb, M. A.; Cheeseman, J. R.; Montgomery, J. A., Jr.; Vreven, T.; Kudin, K. N.; Burant, J. C.; Millam, J. M.; Iyengar, S. S.; Tomasi, J.; Barone, V.; Mennucci, B.; Cossi, M.; Scalmani, G.; Rega, N.; Petersson, G. A.; Nakatsuji, H.; Hada, M.; Ehara, M.; Toyota, K.; Fukuda, R.; Hasegawa, J.; Ishida, M.; Nakajima, T.; Honda, Y.; Kitao, O.; Nakai, H.; Klene, M.; Li, X.; Knox, J. E.; Hratchian, H. P.; Cross, J. B.; Bakken, V.; Adamo, C.; Jaramillo, J.; Gomperts, R.; Stratmann, R. E.; Yazyev, O.; Austin, A. J.; Cammi, R.; Pomelli, C.; Ochterski, J. W.; Ayala, P. Y.; Morokuma, K.; Voth, G. A.; Salvador, P.; Dannenberg, J. J.; Zakrzewski, V. G.; Dapprich, S.; Daniels, A. D.; Strain, M. C.; Farkas, O.; Malick, D. K.; Rabuck, A. D.; Raghavachari, K.; Foresman, J. B.; Ortiz, J. V.; Cui, Q.; Baboul, A. G.; Clifford, S.; Cioslowski, J.; Stefanov, B. B.; Liu, G.; Liashenko, A.; Piskorz, P.; Komaromi, I.; Martin, R. L.; Fox, D. J.; Keith, T.; Al-Laham, M. A.; Peng, C. Y.; Nanayakkara, A.; Challacombe, M.; Gill, P. M. W.; Johnson, B.; Chen, W.; Wong, M. W.; Gonzalez, C.; Pople, J. A.; *Gaussian 03*, Revision C.02; Gaussian, Inc.: Wallingford, CT, 2004.

MeCN for the metal complexes. The activation energy (E_a) of *Z*-to-*E* isomerization, a thermally driven process, has been calculated. The slow rate of isomerization in complexes may be due to a higher rotor volume than that of free ligands.

Crystallographic data for the structure of *trans*-Pd(α-NaiBz)$_2$Cl$_2$ (**7c**) have been deposited with the Cambridge Crystallographic Data center, CCDC No. 689331. Copies of this information may be obtained free of charge from the Director, CCDC, 12 Union Road, Cambridge CB2 1EZ, United Kingdom (e-mail: deposit@ccdc.cam.ac.uk or online at htpp://www.ccdc.cam.ac.uk).

Acknowledgment. Financial support from the University Grants Commission and the Council of Scientific and Industrial Research (CSIR), New Delhi are gratefully acknowledged. We thank National Single Crystal Facility Centre, IISc, Bangalore, India, for there help regarding X-ray crystallographic data collection.

IC8012365

(28) Becke, A. D. *J. Chem. Phys.* **1993**, *98*, 5648.
(29) (a) Hay, P. J.; Wadt, W. R. *J. Chem. Phys.* **1985**, *82*, 270. (b) Wadt, W. R.; Hay, P. J. *J. Chem. Phys.* **1985**, *82*, 284. (c) Hay, P. J.; Wadt, W. R. *J. Chem. Phys.* **1985**, *82*, 299.